

Study of Tritium Production and Interactions in LiD

Serena Fattori*, Rino Persiani†, Ugo Abundo

31st March 2017

Abstract

This study focuses on a fuel cell composed of Lithium Deuteride (LiD) in a spherical geometry, in which isotropic monoenergetic neutrons of 0.025 eV (thermal neutrons) are generated at the center. The objective is to investigate the production of Tritium via interactions with Lithium-6. The physics of the process has been modeled and analyzed for thirteen different concentrations of Lithium-6 to determine the most advantageous option among them. Monte Carlo simulations were performed using the GEANT4 toolkit to analyze neutron interactions and tritium production efficiency as a function of Lithium-6 concentration.

1 Introduction

The purpose of this second phase of the work (for the first part refer to [1]) is to study a fuel cell composed of Lithium Deuteride in a spherical geometry, at the center of which isotropic monoenergetic neutrons of 0.025 eV (thermal neutrons) are generated. The objective is to verify the production of Tritium through reactions with Lithium-6. The physics of the process has been implemented and studied for thirteen different concentrations of Lithium-6 to identify the most efficient among all those considered for comparison.

2 Materials and Methods

The study of neutron interaction processes in Lithium Deuteride, along with the analysis of the fuel cell model, was carried out through Monte Carlo simulations using the GEANT4 toolkit [2], version 10.2.

2.1 Geometry

The studied geometry for the fuel cell consists of a sphere with a point-like neutron source at its center. The sphere's radius is set at 20.0 cm to ensure that all primary neutrons are captured, regardless of the Lithium-6 concentration considered.

Figure 1 illustrates the spatial distributions of the primary neutron interaction points for three cases:

- The first case (large sphere on the left) corresponds to a Lithium-6 concentration of 1% (depleted compared to the natural concentration);

- The second case (medium sphere in the center) represents a natural Lithium-6 concentration of 7.59%;
- The third case (small sphere on the right) corresponds to a Lithium-6 concentration of 100% (maximum enrichment).

These images provide a preliminary qualitative insight: as the Lithium-6 concentration increases, a smaller thickness is required for all primary thermal neutrons to interact within the fuel cell. For quantitative details concerning these three cases and the remaining ten, refer to the subsequent sections of this report.

2.2 Physics

For the interaction modeling, the "High Precision" (HP) mode was selected, as in the previous study on neutron moderation [1]. This choice provides the most realistic description of low-energy processes; however, it comes at the cost of a significant slowdown in interaction execution. For convenience, we recall the neutron physics models activated in this set of simulations, as previously described.

The primary neutron interaction processes considered include:

- Elastic Scattering;
- Inelastic Scattering;
- Capture;
- Fission.

*Email: dr.serena.fattori@gmail.com, ORCID: 0000-0002-9381-7620

†Email: rinopersiani@gmail.com, ORCID: 0000-0002-3100-1466

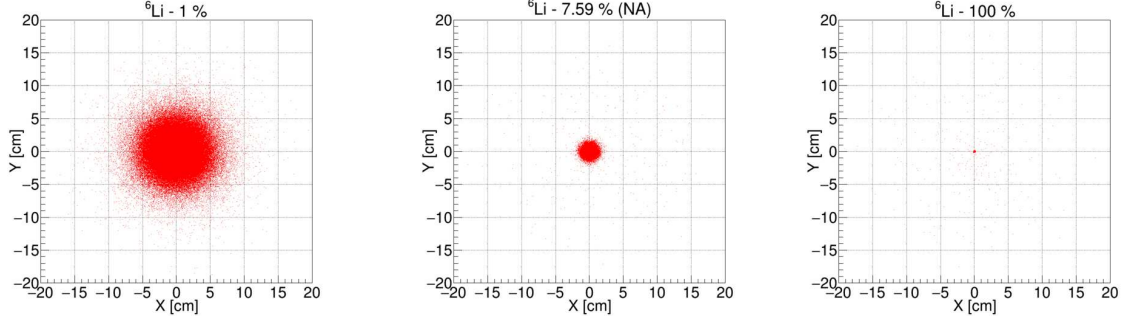


Figure 1: Spatial distributions of primary neutron interaction points in three limiting cases: Lithium-6 concentration at 1% (left image), Lithium-6 concentration at 7.59% (center image), and Lithium-6 concentration at 100% (right image).

Various models were used for different energy ranges, with the "High Precision" mode employed for neutron transport and interactions below 20 MeV, based on experimental data-driven models. The following models were also used [3]:

- hElasticCHIPS: describes hadron-nucleus elastic scattering using M. Kossov's parameterized cross-sections;
- QGSP: "Quark Gluon String model," a theoretical model for high-energy interactions;
- FTFP: models string formation in hadron-nucleus collisions;
- Binary Cascade: generates final states in inelastic hadron scattering;
- nRadCapture: describes neutron capture in the high-energy range;
- G4LFission: models high-energy fission processes.

```
Material: 116 density: 820.066 ng/cm3 RadL: 1.094 m Nucl.int.Length: 47.630 cm
Ineen: 33.394 eV
---- Element: Lithium (Li) Z = 3,0 N = 7 A = 6.941 g/mole
---- Isotope: 116 Z = 3 N = 7 A = 7.02 g/mole abundance: 92.419 %
---- Isotope: 116 Z = 3 N = 6 A = 6.92 g/mole abundance: 7.598 %
ElMassFraction: 77.52 % ElAbundance 50.09 %
---- Element: Deuterium (D) Z = 1,0 N = 2 A = 2.014 g/mole
---- Isotope: 40 Z = 1 N = 2 A = 2.01 g/mole abundance: 100.000 %
ElMassFraction: 22.48 % ElAbundance 50.09 %
```

Figure 2: Image captured from the Terminal during the execution of the simulation: material chemistry.

3 Data and Analysis

3.1 Neutron Interactions in the Fuel Cell

To study Tritium production, 10^6 neutrons of 0.025 eV were generated from the center of a sphere of 20.0 cm radius, composed of Lithium Deuteride. The primary reaction involved is:



The mean kinetic energy available to Tritium is 2.726 MeV, while for the alpha particle, it is 2.055 MeV (as shown in Figures 3 and 4).

The frequency of this inelastic interaction was then studied as a function of the sphere's radius for different Lithium-6 concentrations. The obtained results are illustrated in Figures 5 (for the natural concentration), 6 (for concentrations of 1%, 5%, 10%, 20%, 30%, and 40%), and 7 (for concentrations of 50%, 60%, 70%, 80%, 90%, and 100%). In the images, the contributions to the reaction from primary neutrons are shown in red, while the part of the distribution fed by secondary neutrons is shown in white.

From the analysis of the graphs, it is evident that:

- The contribution from primary neutrons follows an exponentially decreasing trend as a function of distance and drops rapidly (within 2 cm already for the first enrichment considered: 10% Lithium-6);
- The contribution from secondary neutrons remains constant as a function of distance.

The efficiency of this Tritium production process by thermal neutrons was verified as a function of Lithium-6 concentration, leading to the following results: efficiency > 99% for a Lithium-6 concentration of 1%, and efficiency > 99.9% for all other tested concentrations ($\geq 5\%$).

The outgoing neutrons from the fuel sphere and their average energy were then analyzed as a function of Lithium-6 concentration. The results obtained are shown in Figure 8 and Figure 9, respectively. The results clearly indicate that the number of neutrons leaving the sphere decreases as the Lithium-6 concentration increases, while their average energy increases accordingly.

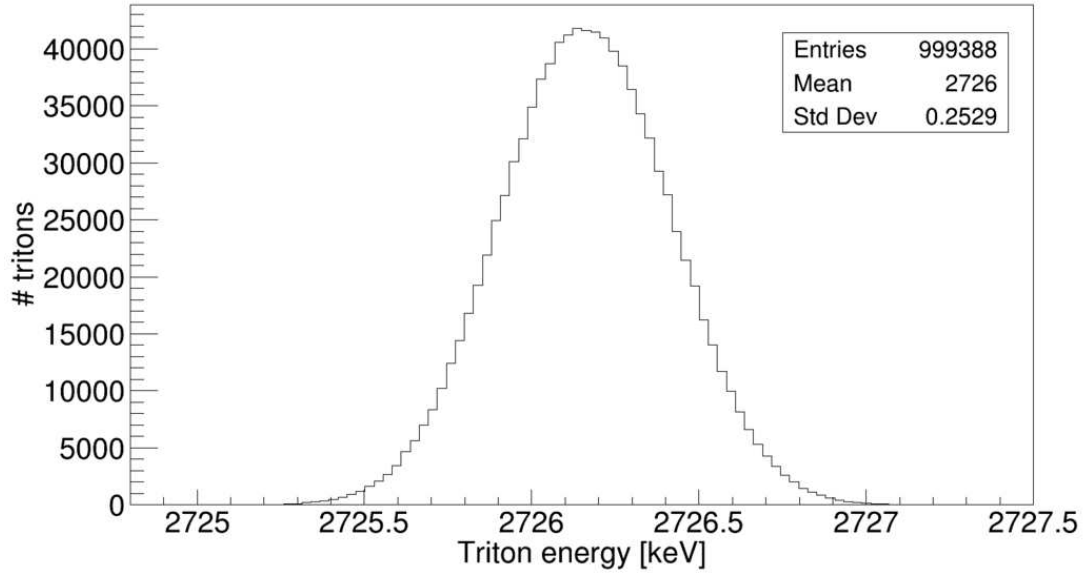


Figure 3: Energy spectrum available to Tritium, produced by the reaction ${}^6\text{Li} + n \rightarrow t + \alpha$.

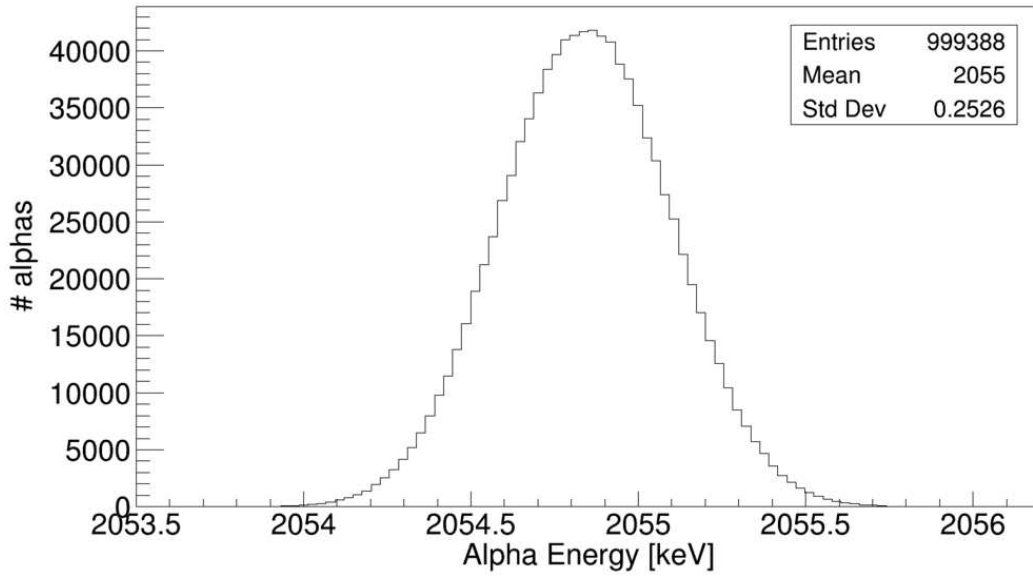


Figure 4: Energy spectrum available to α particle, produced by the reaction ${}^6\text{Li} + n \rightarrow t + \alpha$.

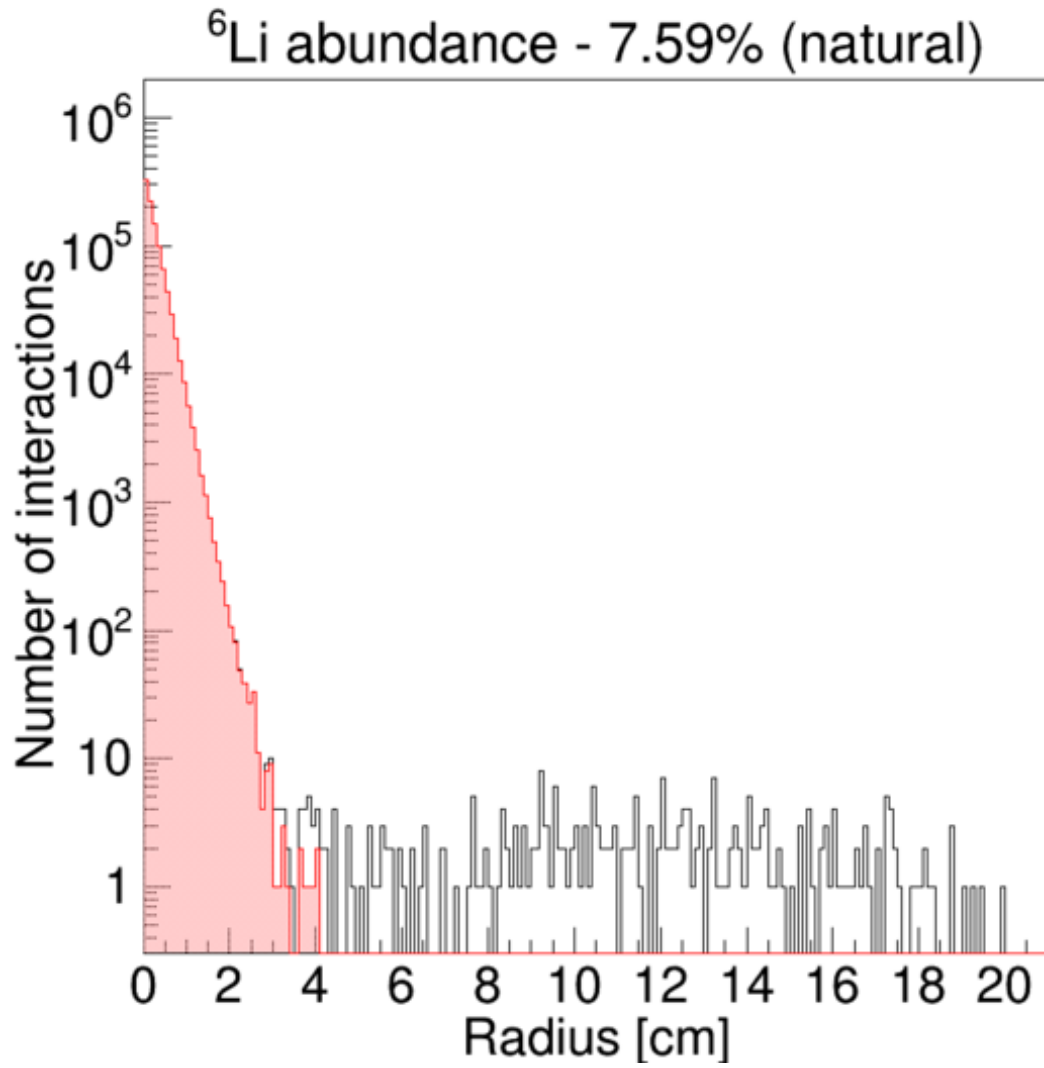


Figure 5: Frequency of the reaction ${}^6\text{Li} + n \rightarrow t + \alpha$ as a function of the fuel sphere radius, for a natural concentration of Lithium-6.

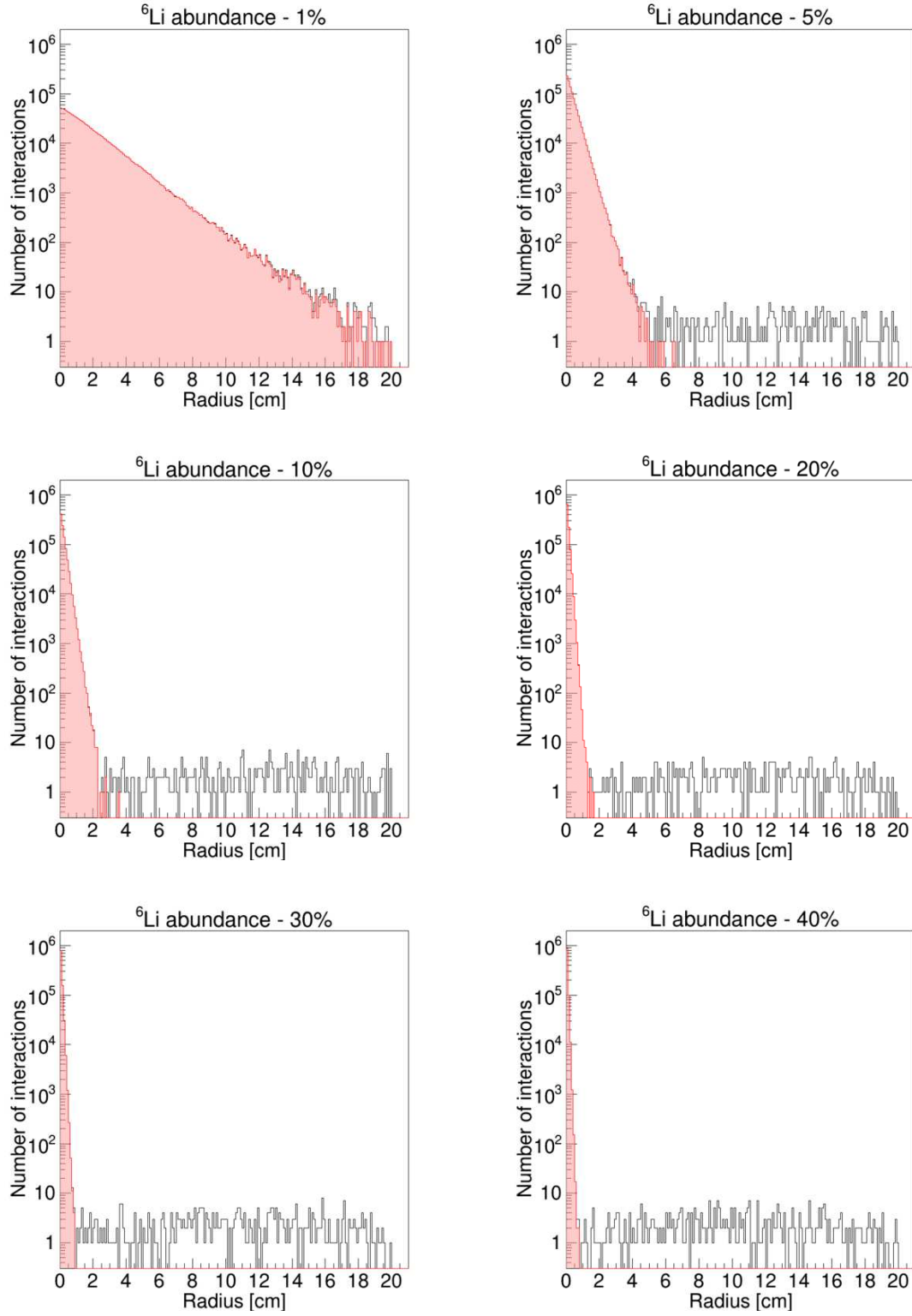


Figure 6: Frequency of the reaction ${}^6\text{Li} + n \rightarrow t + \alpha$ as a function of the fuel sphere radius, for Lithium-6 concentrations of 1%, 5%, 10%, 20%, 30% e 40%.

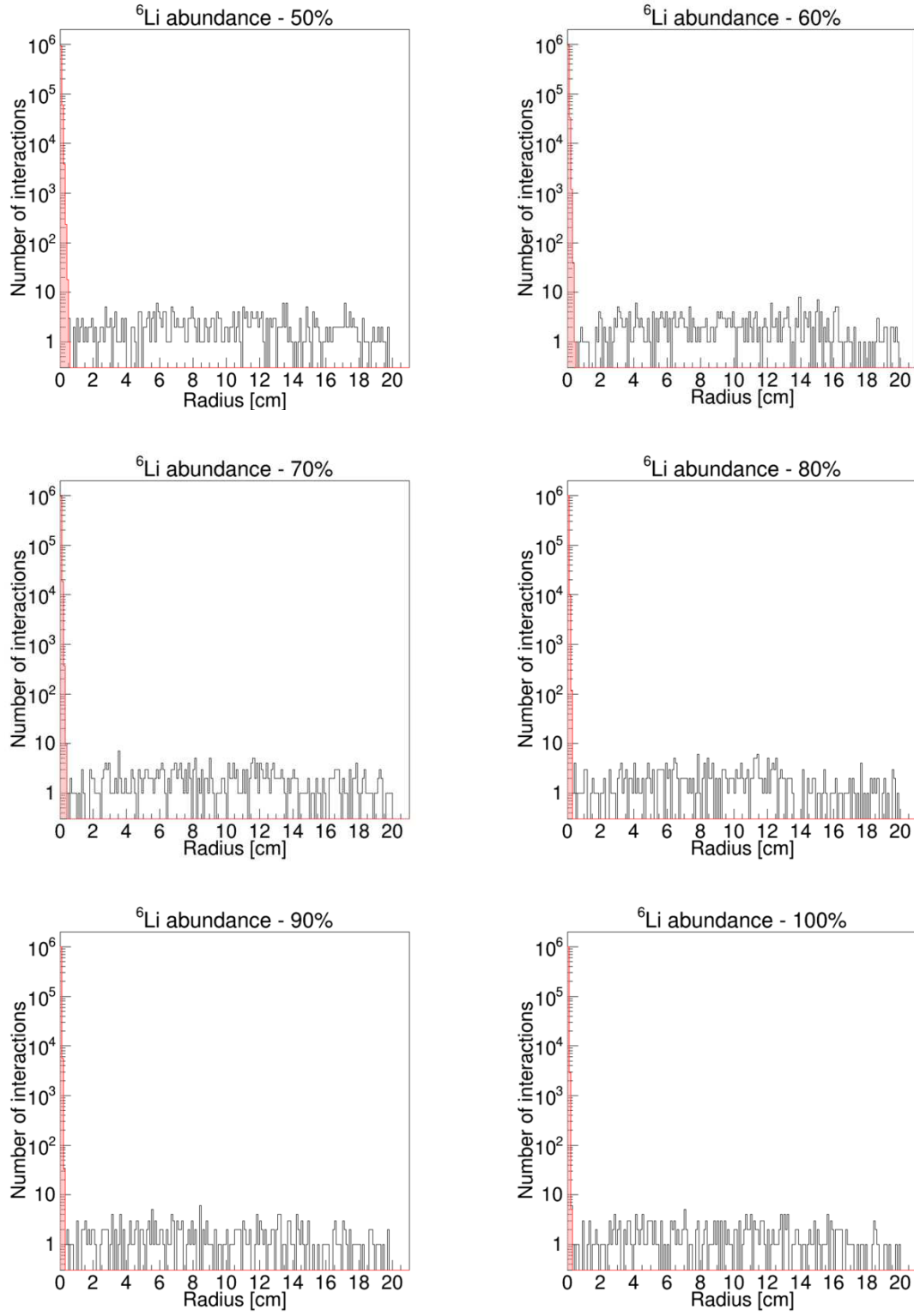


Figure 7: Frequency of the reaction ${}^6\text{Li} + n \rightarrow t + \alpha$ as a function of the fuel sphere radius, for Lithium-6 concentrations of 50%, 60%, 70%, 80%, 90% e 100%.

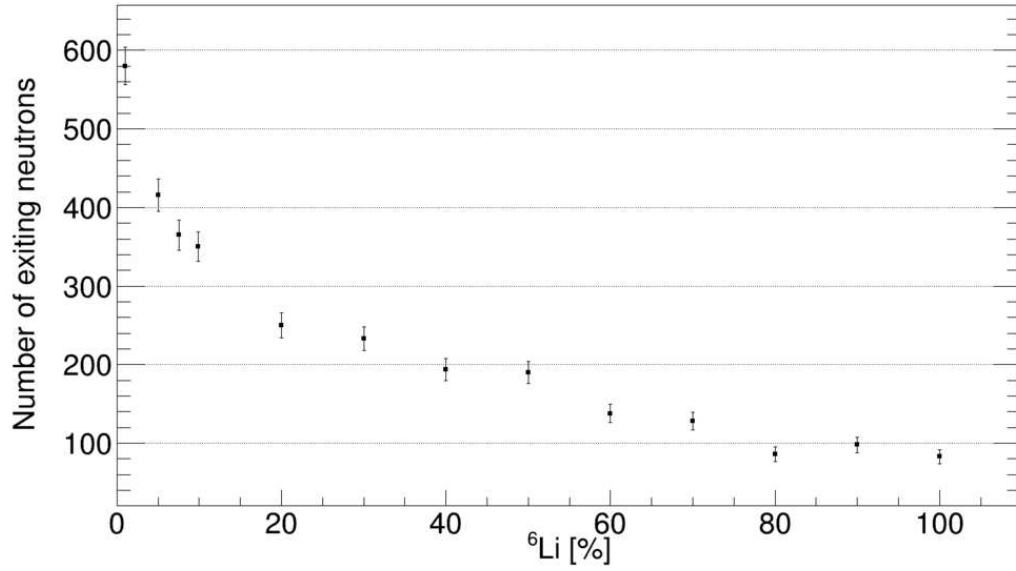


Figure 8: Number of neutrons exiting the fuel sphere as a function of Lithium-6 concentration. Number of primaries generated in all cases: 10^6 .

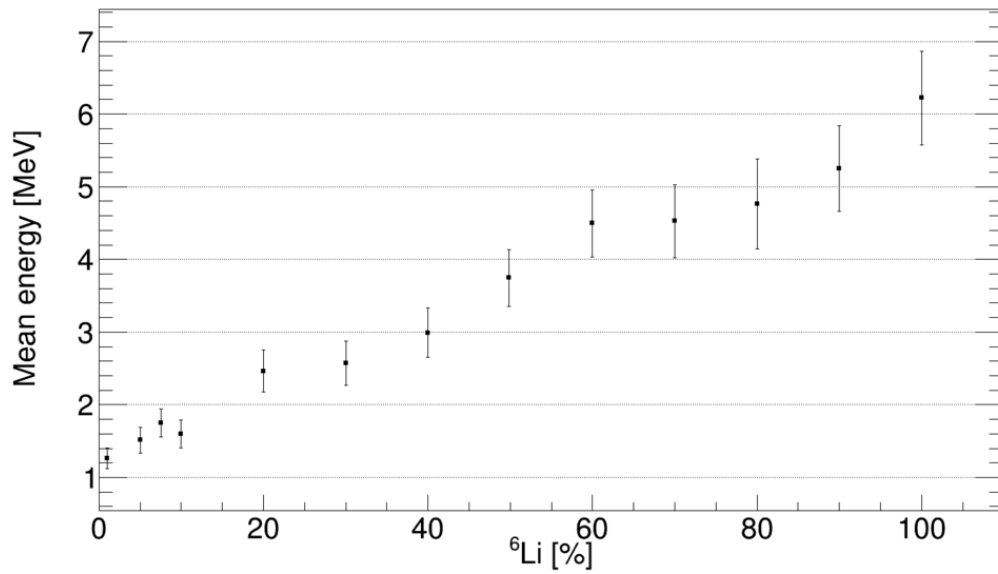


Figure 9: Mean energy of the neutrons exiting the fuel sphere as a function of Lithium-6 concentration.

3.2 Tritium Interaction in the Fuel Cell

The interactions that Tritium can undergo within the fuel cell have also been analyzed. In most cases, it decays after a few elastic scatterings, while in a smaller number of cases, it interacts with Deuterium, Lithium-6, and Lithium-7. The frequencies of these interactions as a function of Lithium-6 concentration are illustrated in Figure 10.

Figures 11, 12, and 13 respectively illustrate, for all interactions combined, as well as for the three most significant interactions:

$$t + d \rightarrow \alpha + n \quad (2)$$

$$t + {}^7\text{Li} \rightarrow 2\alpha + 2n \quad (3)$$

$$t + {}^7\text{Li} \rightarrow \text{other channels} \quad (4)$$

- The total energy available to the reaction products (Figure 11);
- The energy released to α particles (Figure 12);
- The energy released to neutrons (Figure 13).

By analyzing these graphs, one can deduce that Tritium interactions with Deuterium are independent

of the Lithium-6 concentration (see the blue line in Figure 10, keeping in mind that, given the statistics of these events, each point has an error, not represented in the graph, between 5% and 10%). It has been verified that when interaction with Deuterium occurs, the energy available to the reaction products is approximately 19.5 MeV (see the blue distribution in Figure 11), and this energy is shared between the alpha particle and the neutron (see the blue distributions in Figures 12 and 13, respectively).

Another observation from these graphs is that the primary Tritium reaction, occurring in about 55%-60% of cases for a natural concentration of Lithium-6, is with Lithium-7, producing 2 alpha particles and 2 neutrons (see the red line in Figure 10). In this case, the energy available to the reaction products is approximately 10.5 MeV (see the red distribution in Figure 11), and thus the produced alpha particles and neutrons have lower energy compared to the previous case (see the red distributions in Figures 12 and 13, respectively).

Approximately an additional 20% of Tritium interactions occur with Lithium-7 through different channels. In detail, all the observed reactions with the applied statistics (10^6 primary particles generated) are listed in Table 1, along with their percentage frequency as a function of Lithium-6 concentration.

Interaction	${}^6\text{Li}$ concentration [%]												
	1	5	7.59	10	20	30	40	50	60	70	80	90	100
$t + d \rightarrow \alpha + n$	18.3	19.3	19.3	17.2	18.2	16.6	17.7	19.2	17.9	16.5	16.3	15.8	18.7
$t + {}^7\text{Li} \rightarrow 2\alpha + 2n$	65.3	56.4	53.6	59.1	46.4	46.9	40.0	30.7	26.2	19.8	12.1	7.8	0.0
$t + {}^7\text{Li} \rightarrow n + {}^9\text{Be}$	6.6	5.8	7.0	5.8	6.7	5.9	4.7	5.0	1.0	2.3	2.0	1.0	0.0
$t + {}^7\text{Li} \rightarrow \alpha + {}^6\text{He}$	3.0	5.3	4.9	4.3	3.5	2.6	2.2	1.7	2.4	1.6	1.3	0.5	0.0
$t + {}^6\text{Li} \rightarrow d + {}^7\text{Li}$	0.2	1.4	1.0	1.5	2.7	6.2	6.6	7.0	9.0	14.0	14.6	17.1	18.7
$t + {}^6\text{Li} \rightarrow d + \gamma + {}^7\text{Li}$	0.0	0.5	0.8	0.8	2.7	1.9	2.2	5.0	5.5	5.8	5.5	9.8	7.9
$t + {}^6\text{Li} \rightarrow t + {}^6\text{Li}$	0.0	0.0	0.0	1.3	2.1	2.8	2.5	3.6	4.5	4.2	5.0	2.8	6.3
$t + {}^6\text{Li} \rightarrow p + {}^8\text{Li}$	0.0	0.0	1.0	0.3	1.6	1.7	2.9	3.6	3.6	5.3	6.3	5.2	7.5
$t + {}^7\text{Li} \rightarrow t + {}^7\text{Li}$	5.4	7.0	8.0	4.8	5.1	3.8	3.4	2.4	2.1	2.8	0.5	0.5	0.0
$t + {}^6\text{Li} \rightarrow 2\alpha + n$	0.5	2.8	3.9	4.3	10.7	10.7	16.0	19.7	26.4	25.6	34.7	37.5	39.7
$t + {}^7\text{Li} \rightarrow t + \gamma + {}^7\text{Li}$	0.7	1.6	0.3	0.8	0.3	0.7	1.0	1.0	0.7	0.2	0.0	0.3	0.0
$t + {}^6\text{Li} \rightarrow p + \gamma + {}^8\text{Li}$	0.0	0.0	0.3	0.0	0.0	0.2	0.7	1.2	0.7	1.9	1.8	1.8	1.2

Table 1: The table shows the percentage frequencies of all Tritium interactions observed with the given statistics (10^6 primaries generated) as a function of the Lithium-6 concentration in Lithium Deuteride.

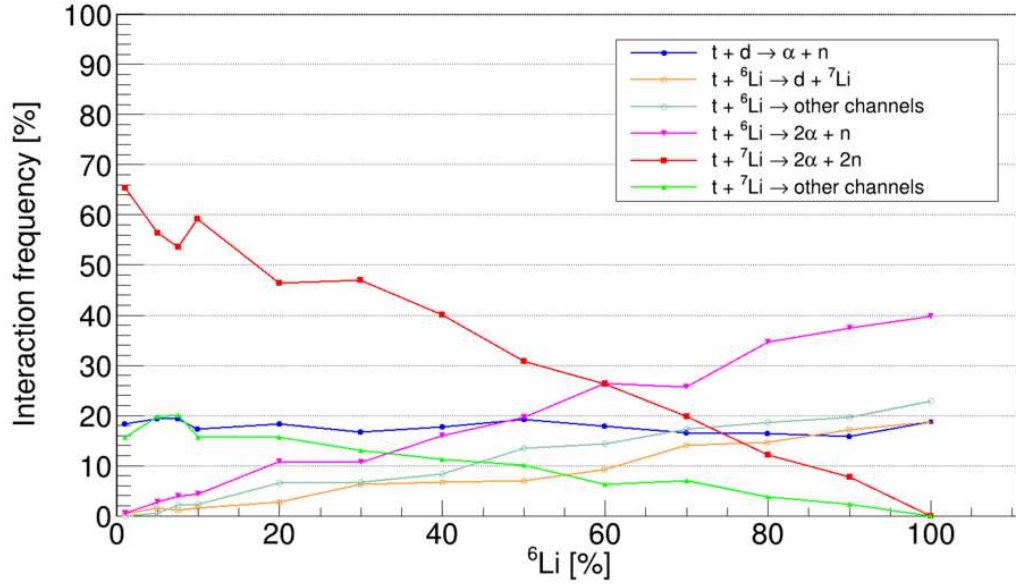


Figure 10: Frequency of various Tritium interactions in Lithium Deuteride as a function of Lithium-6 concentration.

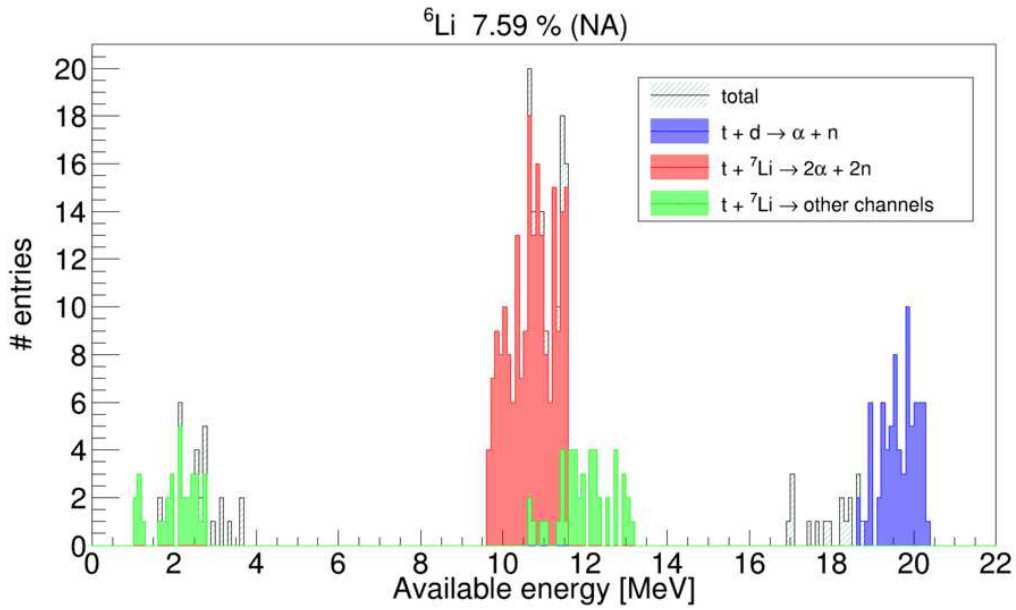


Figure 11: Spectra of the total energy available to the reaction products of the main Tritium reactions in Lithium Deuteride, with Lithium-6 at its natural concentration.

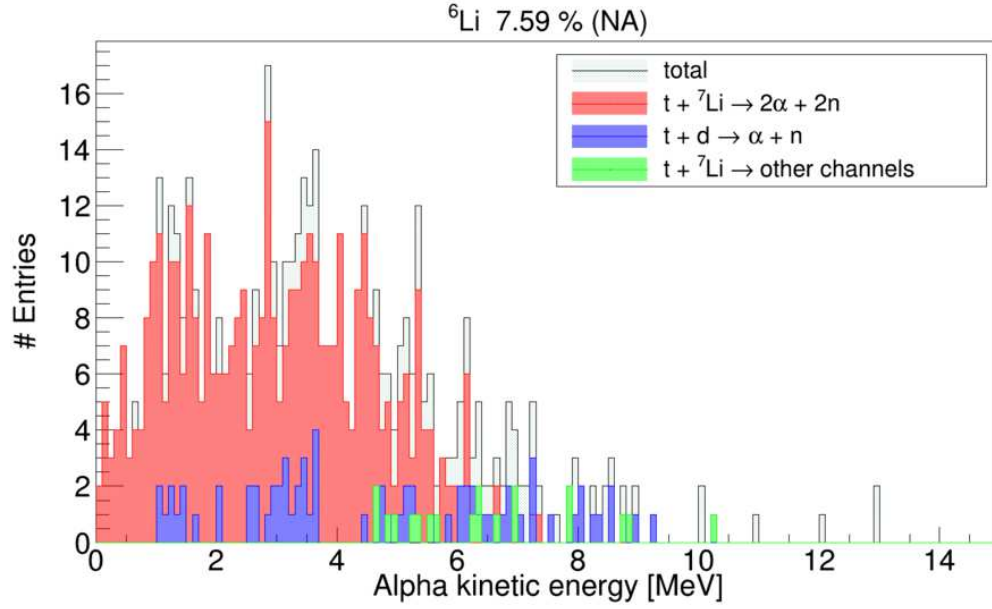


Figure 12: Spectra of the kinetic energy available to the alpha particles produced by the main Tritium reactions in Lithium Deuteride, with Lithium-6 at its natural concentration.

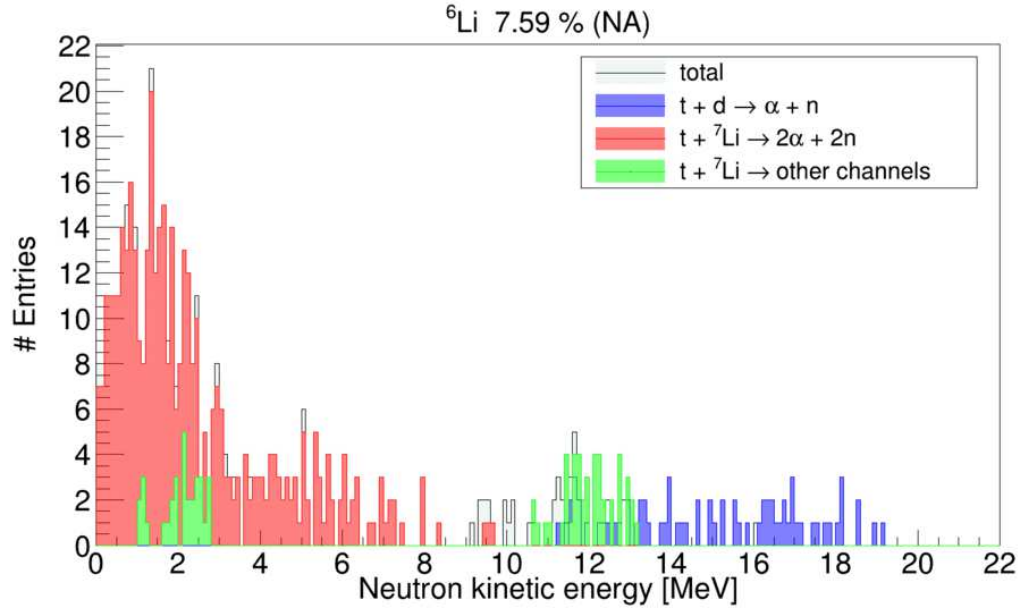


Figure 13: Spectra of the kinetic energy available to the neutrons produced by the main Tritium reactions in Lithium Deuteride, with Lithium-6 at its natural concentration.

4 Conclusions

From the results obtained in this study on the production and interactions of Tritium in Lithium Deuteride, the following considerations can be made:

1. In the first part, where the production of Tritium was analyzed, it was found that all primary neutrons generated are stopped within a few centimeters of the fuel sphere's thickness, even with Lithium-6 at its natural concentration. Moreover, this stopping thickness rapidly decreases as the concentration of Lithium-6 increases. This suggests that it is not essential to achieve high enrichment levels, as even with just 10%-20% of Lithium-6, all primary thermal neutrons are stopped within less than 3 cm;
2. In the second part, where the interactions of the produced Tritium were studied, it was confirmed that the process $t + d \rightarrow \alpha + n$ is, as expected, independent of the Lithium-6 concentration. Therefore, this process does not require enrichment to be sustained. In addition to this process, another significant neutron-producing reaction was identified: $t + {}^7\text{Li} \rightarrow 2\alpha + 2n$, with

an average available energy of approximately 10.5 MeV. Although this energy is lower than the one of the other channel, it occurs with a higher probability.

Acknowledgments

We thank Futureon s.r.l. Centro Ricerche Energetiche, via Acqua Donzella 33, 00179 Rome, for supporting this work.

References

- [1] Serena Fattori, Rino Persiani, Ugo Abundo, *Study of 14.1 MeV Neutron Moderation in Beryllium*, <https://doi.org/10.48550/arXiv.2503.08396> [**nucl-th**].
- [2] S. Agostinelli et al., *Geant4-a simulation toolkit*, [http://dx.doi.org/10.1016/S0168-9002\(03\)01368-8](http://dx.doi.org/10.1016/S0168-9002(03)01368-8) *Nucl. Instr. Meth. A* **506**, (2003).
- [3] Dennis H. Wright et al., *Low and High Energy Modeling in Geant4* AIP Conf.Proc. **896** (2007) 11-20 SLAC-REPRINT-2007-197